Nucleic Acids Research, 2005, Vol. 33, No. 11 ***3529–3539***
doi:10.1093/nar/gki666

Mapping the interaction of SmpB with ribosomes by footprinting of ribosomal RNA

Natalia Ivanova, Michael Y. Pavlov, Elli Bouakaz, Måns Ehrenberg and Lovisa Holmberg Schiavone[1,*]

Department of Cell and Molecular Biology, BMC, Uppsala University, Box 596, S-75 124 Uppsala, Sweden and [1]Cell Biology Unit, Department of Life Sciences, Södertörns Högskola, S-141 89 Huddinge, Sweden

Received April 15, 2005; Revised and Accepted June 6, 2005

ABSTRACT

In *trans*-translation transfer messenger RNA (tmRNA) and small protein B (SmpB) rescue ribosomes stalled on truncated or in other ways problematic mRNAs. SmpB promotes the binding of tmRNA to the ribosome but there is uncertainty about the number of participating SmpB molecules as well as their ribosomal location. Here, the interaction of SmpB with ribosomal subunits and ribosomes was studied by isolation of SmpB containing complexes followed by chemical modification of ribosomal RNA with dimethyl sulfate, kethoxal and hydroxyl radicals. The results show that SmpB binds 30S and 50S subunits with 1:1 molar ratios and the 70S ribosome with 2:1 molar ratio. SmpB-footprints are similar on subunits and the ribosome. In the 30S subunit, SmpB footprints nucleotides that are in the vicinity of the P-site facing the E-site, and in the 50S subunit SmpB footprints nucleotides that are located below the L7/L12 stalk in the 3D structure of the ribosome. Based on these results, we suggest a mechanism where two molecules of SmpB interact with tmRNA and the ribosome during *trans*-translation. The first SmpB molecule binds near the factor-binding site on the 50S subunit helping tmRNA accommodation on the ribosome, whereas the second SmpB molecule may functionally substitute for a missing anticodon stem–loop in tmRNA during later steps of *trans*-translation.

INTRODUCTION

Translation of the genetic information from nucleotide sequences (mRNAs) to amino acid sequences (proteins) takes place on the ribosome—a large ribonucleoprotein complex that consists of two subunits with distinct functions. Bacterial ribosomes (70S) are composed of a small (30S) subunit, containing 16S ribosomal RNA (rRNA) and ~20 ribosomal proteins (r-proteins), and a large (50S) subunit, which contains 23S rRNA, 5S rRNA and more than 30 proteins (1).

Each subunit has three tRNA-binding sites (2): the A (aminoacyl) site, where the incoming aminoacylated tRNA binds; the P (peptidyl) site, where the tRNA with the nascent peptide chain is bound after translocation; and the E (exit) site, from where the deacylated tRNA leaves the ribosome. The molecular interactions of A-, P- and E- site bound tRNAs with the 70S ribosome are revealed in the 3D structure of the mRNA programmed 70S ribosome in complex with tRNAs (1,3). During normal translation, aminoacylated tRNAs are delivered to the decoding centre (DC) in the A-site of the small ribosomal subunit in complex with elongation factor Tu (EF-Tu). EF-Tu binds, similar to other auxiliary GTPase factors in protein synthesis, to the factor-binding site close to the GTPase-activating centre (GAC) of the large subunit. The peptidyl transferase centre in the large ribosomal subunit catalyses peptide-bond formation between the peptide in the P-site and the amino acid in the A-site and then elongation factor G promotes the translocation of the newly formed peptidyl tRNA from the A- to the P-site resulting in an empty A-site, a peptidyl tRNA in the P-site and a deacylated tRNA in the E-site. The newly synthesized proteins are released when the ribosome reaches a stop codon on the mRNA [reviewed in (4)].

During *trans*-translation (5,6), a hybrid transfer-messenger RNA (tmRNA) molecule and its helper protein SmpB (small protein B) rescue ribosomes stalled on truncated mRNAs lacking stop codons. tmRNA possesses a tRNA-like domain (TLD), which is aminoacylated with alanine (7,8) and an mRNA-like domain, containing an internal open reading frame (ORF) (9) encoding a proteolysis tag (10). tmRNA, charged with alanine and in complex with EF-Tu (11–13) and SmpB (12,14,15), binds to the empty A-site of a stalled ribosome. The nascent polypeptide on the P-site tRNA of the ribosome is then transferred to the Ala-tmRNA and *trans*-translation resumes on the internal ORF of tmRNA (10). Eventually, a protein marked for degradation (16) is released, allowing the ribosome to recycle back to a new round of initiation (17).

*To whom correspondence should be addressed. Tel: +46 8 6084597; Fax: +46 8 6084510; Email: lovisa.holmberg-schiavone@sh.se

SmpB is the only known protein co-factor of tmRNA, which is essential for *trans*-translation (14,18). It is a small protein with a globular β-barrel domain and a basic C-terminal tail similar to that of ribosomal protein S17 (19,20). The β-barrel domain has an extended oligonucleotide-binding (OB) fold with basic residues concentrated to opposing surfaces (19). It has been suggested that SmpB uses those surfaces to interact simultaneously with tmRNA and 16S rRNA serving as a bridge between them (21). It has been shown that although a tail-truncated SmpB binds both to the ribosome and to tmRNA with high affinity, it cannot support *trans*-translation (21). As discussed below, the C-terminal tail of SmpB is suggested to assist in Ala-tmRNA accommodation into the 70S A-site by extending into the DC and mimicking a missing codon–anticodon interaction between tmRNA and the ribosome (21,22).

A high-resolution crystal structure of a complex containing SmpB and the TLD of tmRNA from *Aquifex aeolicus* (22) reveals that one side of the OB fold in SmpB binds to the elbow region of the TLD and stabilizes its D-loop in an extended conformation. The C-terminal tail of SmpB is disordered and cannot be traced in the crystal structure (22). Cross-linking to and footprinting on tmRNA by SmpB [(12,23); N. Ivanova, M. Lindell, M. Pavlov, L. Holmberg Schiavone, E.G.H. Wagner and M. Ehrenberg, manuscript in preparation] confirm that SmpB interacts with the D- and connector-loops of the TLD.

In the cell SmpB is predominantly ribosome-bound, independently of the presence of tmRNA, suggesting that SmpB could be associated with ribosomes at other times than during *trans*-translation (21,24). Existing data indicate that SmpB may be in complex with tmRNA during the entire *trans*-translation cycle on the ribosome [(25); N. Ivanova, M. Lindell, M. Pavlov, L. Holmberg Schiavone, E.G.H. Wagner and M. Ehrenberg, manuscript in preparation], but it is still uncertain how many copies of SmpB bind to the ribosome and tmRNA during *trans*-translation. The cryo-EM structure of the kirromycin-stalled tmRNA•SmpB•EF-Tu•ribosome complex only shows one molecule of SmpB (15), whereas biochemical studies indicate that ribosomes (24) and tmRNA (23,26) can bind two and three SmpB molecules, respectively.

The cryo-EM structure suggests that SmpB interacts primarily with the 50S subunit, whereas tmRNA interacts with the GAC of the 50S subunit and the DC of the 30S subunit (15). At the same time, modelling of the SmpB•TLD crystal structure into the map of the 70S ribosome suggests that SmpB is oriented towards the DC of the small ribosomal subunit (22). To reconcile these two structural models, it has been suggested that SmpB re-orients during the accommodation of tmRNA into the ribosomal A-site (22). In this model, SmpB would first bind to the factor-binding site of the 50S subunit as seen in the cryo-EM structure. Then, upon accommodation of tmRNA into the ribosomal A-site, SmpB would be reoriented to the DC of the small ribosomal subunit and use its C-terminal tail to substitute for the lack of anticodon stem–loop (ASL) in tmRNA (15,21,22,25). It has also been proposed that SmpB should dissociate from tmRNA at later stages of *trans*-translation upon peptidyl-tmRNA translocation to the P-site of the ribosome to make room for the entry of a native aminoacyl-tRNA into the A-site (22).

The absence of consensus regarding the mode of the interaction between SmpB and the ribosome prompted us to characterize interactions of free SmpB with ribosomal subunits and ribosomes. To this end, SmpB containing ribosomal complexes isolated by gel-filtration were probed by chemical modification and hydroxyl radical cleavage of ribosomal RNA. The results show that 70S ribosomes contain two binding sites for SmpB, one close to the P-site of the small subunit and one near the factor-binding site of the large subunit. This observation suggests that two different SmpB molecules participate in *trans*-translation. Comparison of SmpB-footprints with the known position of SmpB on the 50S subunit (15) and with interaction sites of P- and E-site tRNAs in 16S rRNA (1) sheds new light on the function of SmpB in *trans*-translation.

MATERIALS AND METHODS

Materials

His-tagged, and [^{35}S]labelled SmpB was purified from the BL21(DE3)/pet-21a-SmpB *Escherichia coli* strain as described previously (27). Synthetic mRNA, encoding the tetra-peptide Met-Phe-Thr-Ile was prepared by *in vitro* T7 RNA polymerase transcription of the PCR-amplified DNA sequence (28). [^{3}H]fMet-tRNA^{fMet} was prepared from bulk tRNA as described previously (29). tRNA^{Phe} andtRNA$^{Leu}_{GAG}$ isoacceptors were purified on BD-sepharose as described previously (30). Initiation factors were purified from overproducing strains as described previously (29). PheRS, LeuRS and elongation factors EF-Tu and EF-Ts were purified as described previously (31).

Dimethyl sulfate (DMS) and ammonium iron (II) sulfate hexa hydrate were from Acros Organics, NJ. Kethoxal was from MP Biomedicals (Aurora, OH). Hydrogen peroxide was from Fisher Chemicals (Leicester, UK). Ascorbic acid was from Sigma–Aldrich (Steinheim, Germany). Superscript reverse transcriptase was from Life Technologies Inc. (Carlsbad, CA). Deoxy nucleotides were from Roche Diagnostics GmbH (Mannheim, Germany). Ready Protein Plus scintillation liquid was from Beckman Coulter (Fullerton, USA). GeneScan 500XL TAMRA internal size standard was from Applied Biosystems (Warrington, UK).

Primers, labelled at the 5′ end with the fluorescent molecule Blue 6-FAM, were from Cybergene (Huddinge, Sweden). The sequences of the primers (32,33) were the following:

16S: 5′-GCT AAT CCC ATC TGG GC-3′ (232), 5′-TTC TGC GGG TAA CGT CA-3′ (480), 5′-GCA TTT CAC CGC TAC AC-3′ (683), 5′-CCG AAC TGT CTC ACG AC-3′ (906), 5′-ACA GCC ATG CAG CAC CT-3′ (1046), 5′-GCT CTC GCG AGG TCG CT-3′ (1257) and 5′-ACC TTG TTA CGA CTT CA-3′ (1490).

23S: 5′-TCG CCG CTA CTG GGG GA-3′ (235), 5′-TCC CTC ACG GTA CTG GT-3′ (454), 5′-ATC ACC GGG TTT CGG GT-3′ (670), 5′-GAT GAC CCC CTT GCC GA-3′ (872), 5′-ATG ACT TTG GGA CCT TA-3′ (1001), 5′-GCG TCG CTG CCG CAG CT-3′ (1156), 5′-GGCCTCGCCTTAGGGGT-3′ (1347), 5′-GTC GGT TTG GGG TAC GA-3′ (1599), 5′-CCT TCC GGC ACC GGG CA-3′ (1834), 5′-TCC GTC TTG CCG CGG GT-3′ (2042) and 5′-CCT TCG TGC TCC TCC GT-3′ (2274).

5′-TGT TAT CCC CGG AGT AC-3′ (2437, 23S rRNA), 5′-CCG AAC TGT CTC ACG AC-3′ (2592), 5′-GAA CTC ATC

TCG GGG CA-3′ (2769), 5′-AGG TTA AGC CTC ACG GT-3′ (2887) and 5′-ATG CCT GGC AGT TCC CT-3′ (5S rRNA).

Ribosomes and ribosomal subunits

Tight couple 70S ribosomes and ribosomal subunits were prepared from the *E.coli* wild-type MRE 600 strain using sucrose gradient zonal ultracentrifugation following the procedure described previously (34) with the following modifications. Crude ribosomes were isolated, washed twice with 0.5 M NH_4Cl, pelleted (34) and dissolved in buffer C containing [20 mM Tris, pH 7.5, 60 mM NH_4Cl, 5.25 mM $Mg(OAc)_2$, 0.25 mM EDTA and 3 mM 2-mercaptoethanol]. To obtain 70S tight couples, the washed ribosomes were further purified by zonal centrifugation in a Beckman Ti 15 rotor equipped with reo-grad core (Beckman Coulter). The rotor was loaded by pumping 200 ml buffer C (overlay), followed by 40 ml of ribosomal solution in buffer C from the previous step. After this, 1.1 litre of a convex exponential gradient from 10 to 37% sucrose in buffer C was loaded into the rotor followed by 100 ml of 50% sucrose cushion in buffer C. After centrifugation at 4°C for 9 h at 32 000 r.p.m. in the Optima 100 K Ultracentrifuge (Beckman Coulter) the reo-grad rotor was unloaded, 10 ml fractions were collected and the fractions containing 70S ribosomes (tight couples) were identified by absorbance at 260 nm and pooled. Pooled 70S tight couples were recovered by pelleting in a Ti 50.2 rotor (Beckman Coulter) for 30 h at 45 000 r.p.m. Pelleted 70S tight couples were dissolved in polymix buffer, aliquoted in Eppendorf tubes, shock-frozen in liquid nitrogen and stored at −80°C. The activity of the tight couple ribosomes in the fMet-Phe dipeptide formation assay was at least 80% (see Results).

To prepare ribosomal subunits, the pelleted 70S tight couples were dissolved in buffer S containing [20 mM Tris, pH 7.5, 300 mM NH_4Cl, 3 mM $MgCl_2$, 0.5 mM EDTA and 3 mM 2-mercaptoethanol] to which 5% sucrose was added. The Ti 15 rotor with reo-grad core was loaded in the same way as described above but the overlay contained buffer S and 1.1 litre of a convex exponential 7.5–34% sucrose gradient in buffer S was loaded. Centrifugation was again at 4°C for 9 h at 32 000 r.p.m. After unloading the rotor, the 50S and 30S peaks were identified by UV, 50S and 30S fractions were pooled separately and recovered by pelleting in a Ti 50.2 rotor for 36 h at 45 000 r.p.m. Pellets were dissolved in polymix buffer, aliquoted in Eppendorf tubes, shock-frozen in liquid nitrogen and stored at −80°C.

Formation of SmpB containing ribosomal complexes

SmpB containing complexes were formed by incubating SmpB (100–200 pmol) with ribosomal subunits or ribosomes (40 pmol) in TMK-buffer containing [5 mM $Mg(OAc)_2$, 50 mM KOAc and 50 mM Tris–OAc, pH 7.6] in a final volume of 80 µl for 5 min at 37°C. Control samples, without SmpB, were incubated in parallel. Samples were left on ice for 10 min after the incubation.

Stoichiometry of SmpB binding to 70S ribosomes and ribosomal subunits

Stoichiometry of SmpB binding to subunits and ribosomes was estimated in gel-filtration experiments using a 60 ml Sephacryl S300 column (1.6 cm internal diameter and 30 cm length) equilibrated with TMK or polymix buffer containing [5 mM $Mg(Oac)_2$, 0.5 mM $CaCl_2$, 5 mM NH_4Cl, 95 mM KCl, 8 mM putrescine, 1 mM spermidine, 5 mM potassium phosphate (pH 7.3) and 1 mM dithioerythritol (35)]. Complexes were formed as described above using 400 pmol subunits or ribosomes and 1000 pmol [^{35}S]labelled SmpB in a final volume of 0.5 ml of TMK or polymix buffer. Samples were eluted at 1.2 ml/min and 1.2 ml fractions were collected. The amount of SmpB in the fractions was measured by scintillation counting and the concentration of ribosomes was determined from UV measured at 260 nm. In some experiments, 1000 pmol of $tRNA^{Phe}$ or bulk tRNA from *E.coli* was included to check the specificity of tmRNA binding to ribosomes.

Chemical modification with DMS and kethoxal

Free ribosomes or ribosomal subunits and SmpB containing complexes were modified with DMS (final concentration 25 mM) or kethoxal (final concentration 18 mM) for 5 min at 37°C in TMK buffer. Both the DMS and the kethoxal were diluted in ethanol before use. Control samples lacking modifying reagent were incubated in parallel. The kethoxal-adduct was stabilized with 25 mM K-borate (pH 7.0) at all times. Reactions were stopped by EtOH precipitation as described previously (32).

Generation of hydroxyl radicals

Hydroxyl radicals were generated as described previously (36). Briefly, 1 µl of a solution containing 200 mM EDTA (pH 8.0) and 100 mM ammonium iron (II) sulfate was added to the side of an eppendorf tube, containing ribosomal complex or free ribosomes. One µl of a solution consisting of 0.25 M ascorbate and 2.5% H_2O_2 was added to another side of the tube and the samples were mixed by brief spinning in an eppendorf centrifuge at 4°C. The samples were kept on ice for 10 min and then the reactions were quenched by the addition of 1 vol of 0.1 M thiourea.

RNA extraction, primer extension analysis and evaluation of data

RNA was extracted from protein as described previously (32). The positions of the modified sites were identified by primer extension as described previously (37). The primer extension products were analyzed on 5% (w/v) polyacrylamide sequencing gels in an Applied Biosystems 377 DNA sequencer, using an internal size standard, as described previously (37,38). At least three independent modification experiments were performed and analyzed before the data were evaluated. We cannot distinguish between a direct interaction of SmpB with a section of rRNA and conformational changes induced by the interaction of SmpB with the subunit/ribosome by the footprinting technique. However, based on the mapping of SmpB-footprinted nucleotides on the 3D models of 16S rRNA and 23S rRNA [1PNS and 1PNU PDB files (3)], we infer that several footprints are the result of a direct interaction of SmpB with rRNA (see Results).

Dipeptide formation assay

All experiments were carried out in polymix buffer. Two mixes were prepared. The ribosomal mix contained 2.5 µM 70S ribosomes (~2 µM active), 4 µM [^{3}H]fMet-$tRNA^{fMet}$,

4 μM mRNA coding for MFTI tetrapeptide (39), 2 μM each IF1, IF2 and IF3, 1 mM GTP and 4 μM SmpB when specified. The factor mix for the cognate reaction contained 2 μM $tRNA^{Phe}$, 2 μM EF-Tu, 0.2 μM EF-Ts, PheRS (0.5 U/μl), 400 μM phenylalanine, 2 mM ATP, 20 mM PEP, 1 mM GTP, PK (2 μg/ml) and MK (0.2 μg/ml). The factor mix for the near cognate reaction contained 20 μM RNA^{Leu}_{GAG}, 20 μM EF-Tu, 2 μM EF-Ts, LeuRS (0.5 U/μl), 400 μM leucine, 2 mM ATP, 20 mM PEP, 1 mM GTP, PK (2 μg/ml) and MK (0.2 μg/ml). Both the ribosome and the factor mixes were pre-incubated for 10 min at 37°C, mixed in equal volumes, incubated for varying times and quenched by formic acid to a final concentration of 17%. The cognate reaction was carried out with a quench-flow instrument (Chemical-Quench-Flow ModelQF-3, KinTek Corp.). Dipeptide formation was quantified by high-performance liquid chromatography (HPLC) with on-line radio-detection (βRAM3; INUS Inc., USA) from the ratio of the area of the peak of the [^{3}H]fMet-Phe (or [^{3}H]fMet-Leu) dipeptide and the sum of the areas of the dipeptide and [^{3}H]fMet peaks. Samples for the HPLC were prepared and processed as described previously (39).

RESULTS

Here, we have searched for possible interaction sites between the ribosome-associated protein SmpB and ribosomal RNA by chemical modification and subsequent primer extension analysis of SmpB containing or SmpB-free ribosomes and ribosomal subunits.

Binding of SmpB to 30S, 50S and 70S particles

Ribosomal complexes containing SmpB were formed by incubating ribosomes or ribosomal subunits with 2.5- or 5-fold excess of SmpB over ribosomes/subunits in TMK buffer containing 5 mM $Mg(OAc)_2$. The resulting complexes were purified from unbound protein by gel-filtration chromatography on a Sephacryl S-300 column. Figure 1 shows the elution profile of the complexes formed between [^{35}S]labelled SmpB and either 30S, 50S or 70S particles. The results in Figure 1A clearly show that the 70S ribosome could accommodate two molecules of SmpB in agreement with earlier data (24).

The 30S and 50S subunit bound 0.8 and 0.6 molar equivalents of SmpB, respectively (Figure 1B and C). From the elution profiles, it is also apparent that SmpB was present in small amounts in all fractions following the major elution peak containing 30S, 50S or 70S ribosomes. This indicates continuous dissociation of SmpB from complexes while they moved through the gel-filtration column. The amount of dissociated SmpB was significantly larger for 50S•SmpB than for 30S•SmpB complexes and was very small for the 70S•SmpB complex, indicating tighter SmpB binding to the 70S ribosome than to the ribosomal subunits. From these experiments, we concluded that SmpB bound both to the 30S and 50S subunits in a 1:1 molar ratio and to 70S ribosomes in a 2:1 molar ratio. The results shown in Figure 1 were reproducible in different buffer systems, including polymix buffer and the TMK buffer used in the chemical modification experiments. Moreover, the addition of pure $tRNA^{Phe}$ or bulk tRNA from *E.coli* in a 2–5 molar excess over ribosomes or subunits before the application of the SmpB containing complexes to the column did not affect the stoichiometry of SmpB in the complexes after elution from the column (data not shown). This observation shows that SmpB binding to 70S ribosomes and to subunits was specific.

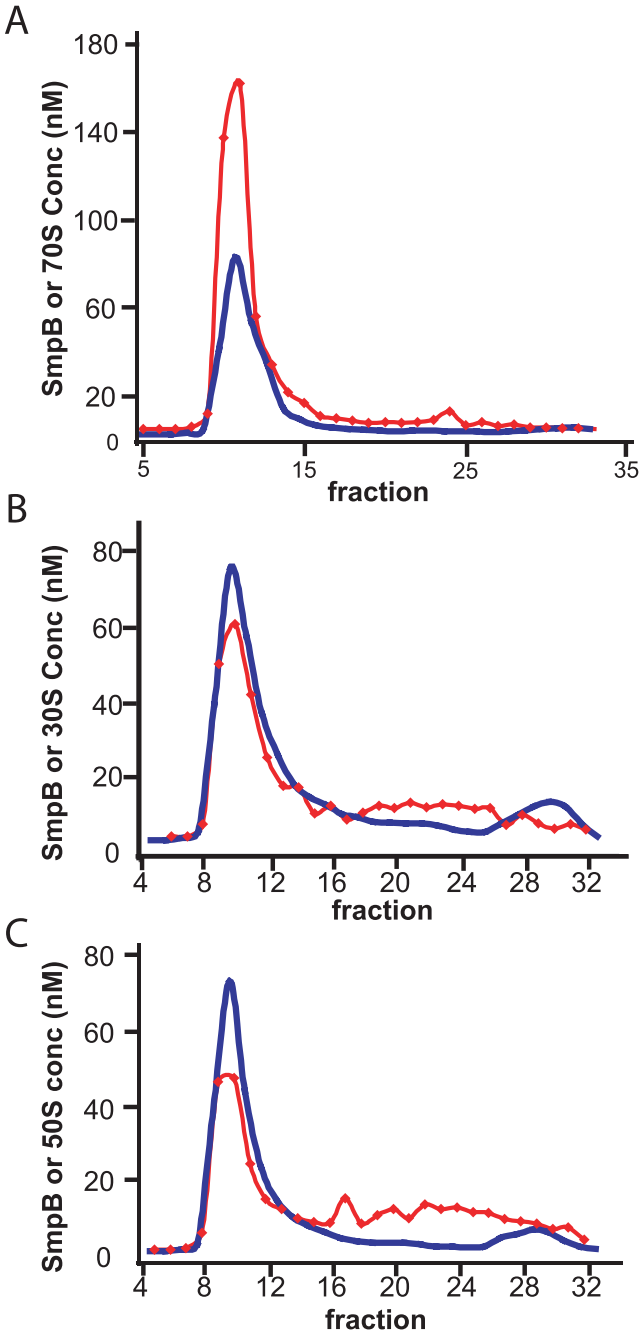

Figure 1. Elution profile of SmpB in complex with 70S ribosomes (**A**) and SmpB in complex with 30S (**B**) or 50S (**C**) ribosomal subunits. Complexes were prepared by mixing 2.5–5 molar excess of SmpB with 70S ribosomes or subunits and loaded onto the Sephacryl S300 gel filtration column. Concentrations of ribosomes and subunits (blue line) in the fractions were determined from UV at 260 nm, while the concentration of [^{35}S]labelled SmpB (red line) was determined by scintillation counting. Free SmpB elutes around fraction 24 from this column.

Footprinting of ribosomal RNA

Ribosomal RNA in SmpB containing complexes or in free subunits/ribosomes was modified with DMS or kethoxal or cleaved with hydroxyl radicals generated from Fe(II)–EDTA. The single-strand specific reagent DMS modifies unpaired As at the N-1 position and unpaired Cs at the N-3 position, whereas kethoxal modifies unpaired Gs at the N-1 or N-2 positions (36). Free hydroxyl radicals are not base-specific but instead induce strand scissions in the sugar–phosphate backbone (36). The modified or cleaved nucleotides were identified by primer extension and gel electrophoresis using an ABI 377 sequencer.

All of 23S, 5S and 16S rRNA, except their 3′ ends, were analysed and the modification patterns of rRNA in SmpB-containing complexes were compared with those in SmpB-lacking complexes. The results show that SmpB protected bases/the sugar–phosphate backbone in specific regions in 16S rRNA, located to its central and 3′-major domains. In 23S rRNA, the backbone was protected in defined regions of domains II, V and VI. The results are summarized in the proposed secondary structure models of 16S and 23S rRNA (Figure 2A and B). The reactivity of nucleotides was affected to a different extent by the binding of SmpB to ribosomes or subunits.

In general, the presence of SmpB reduced the reactivity of bases or the phosphate backbone by 30–70%. The reduction was stronger in 16S than in 23S rRNA, as to be expected from the higher affinity of SmpB for the 30S than for the 50S subunit (Figure 1).

Footprinting of 16S rRNA in 30S subunits and 70S ribosomes

SmpB footprinted nucleotides in the central (Figure 3A–C) and 3′-major (Figure 3D and E) domains in the 16S rRNA. The strongest hydroxyl radical footprints are seen in the 790-loop and connecting helix H24 in the backbones surrounding positions 776–778, 784–787, 790–795, 798–802 and 807–809 (Figure 3A). The largest reduction in reactivity (by 70%) by the association of SmpB to the 30S subunit is seen for positions 785–787. Moreover, in the loop, G791 was protected from kethoxal modification (Figure 3B), whereas A790, A794 and C795 were weakly protected from DMS modification by the formation of SmpB•30S complexes (Figure 3C). Another position in the central domain that was affected in the complexes was G693 in the 690-loop (Figure 3B). Two peaks were seen in this region of the fluorogram, probably due to stuttering of the reverse transcriptase at G693 since the adjacent base is a uracil that should not be accessible for kethoxal modification.

In the linker region (helix H27) between the central and 3′-major domains, bulging nt G926 and G927 were protected from kethoxal modification (Figure 3D). G927 base pairs with U1390 but this does not exclude modification at the N-2 position by kethoxal. The backbone connecting helices H30 and H31 (positions 954–959) was protected from cleavage by the free hydroxyl radicals in the SmpB•30S complex (Figure 3E). Finally, the N-3 position of C1400 in the 3′-minor domain of 16S rRNA became more exposed to DMS modification within the SmpB-containing complex (Figure 3F).

No additional footprints were seen in 16S rRNA in 70S ribosomes. Instead, the reactivity of several nucleotides decreased or disappeared as a result of the interaction of the 50S subunit with the 30S subunit. Thus, the hydroxyl radical cleavages in H24 and its apical 790-loop were abolished by the association of subunits into ribosomes [data not shown; (1,40)]. Moreover, the DMS- and kethoxal-reactivity of A790 and G791, respectively, in the 790-loop disappeared upon the formation of 70S ribosomes (Figure 3B) (1,40), whereas the DMS-reactivity of A794 and C795 was less affected. These 2 nt were footprinted by the association of SmpB with the 70S ribosome (Figure 3C).

Also, hydroxyl radical cleavages in the backbone surrounding positions 954–959 in the 30S subunit disappeared upon 70S formation. Nucleotides 954–959 do not contact the 50S subunit in the crystal structure of the 70S ribosome (1), suggesting that their loss of reactivity was due to a conformational change of the 30S subunit.

The SmpB-footprints in the 690-loop, at G693 (Figure 3B) and at positions G926 and G927 in helix H27 (Figure 3D), were similar in the 70S ribosome and the 30S subunit. Moreover, the reactivity of C1400 was also increased in the SmpB•70S complex compared with ribosomes lacking SmpB (Figure 3F).

Footprinting of 23S rRNA in 50S and 70S particles

We failed to find any base-specific footprints in 23S rRNA in the 50S subunit even at a 5-fold molar excess of SmpB over ribosomes. Instead, the phosphate backbone was protected in three regions from hydroxyl radical cleavage by SmpB (Figure 2B). The reactivity was reduced by 30–50% in the SmpB•50S complex compared with the empty subunit. In helix H89 and its apical loop in domain V, the backbone around positions 2470–2474 was protected from cleavage when SmpB was bound to the 50S subunit (Figure 4A). The footprint was centred on nt U2473 in the 2475-loop. The second protected region was the α-sarcin/ricin-loop in domain VI, positions 2655–2656 and 2661–2664 (Figure 4B). Here, the backbone surrounding U2656 was most strongly affected. Finally, the backbone surrounding nt U1065–A1067, A1073–C1075 in the apical loop of helix H43 and A1095 in the apical loop of helix H44 of domain II was less accessible to the hydroxyl radicals when SmpB was present (Figure 4C). In this case, the footprint was centred on nt A1067.

SmpB-footprints were slightly stronger in the 1070- and 1095-regions in the 70S ribosome compared to in the 50S subunit (Figure 4C). The accessibility of the 2475-loop was reduced in the 70S ribosome compared with the 50S subunit but the SmpB-footprint was similar (Figure 4A). In contrast, the SmpB-footprint in the α-sarcin/ricin-loop was missing in the SmpB•70S complex (Figure 4B).

Mapping of the footprints to the molecular models of 16S and 23S rRNA

The SmpB-footprints were mapped to the 3D structures of 16S and 23S rRNA from the *E.coli* ribosome (3). The footprinted nucleotides in 16S rRNA in the 690- and 790-loops, in helix H24, in the linker region between the central and 3′-major domains (helix H27) and in the single-strand region connecting helices H30 and H31 are located to the platform and the neck region of the 30S subunit (Figure 5A). Interestingly, the

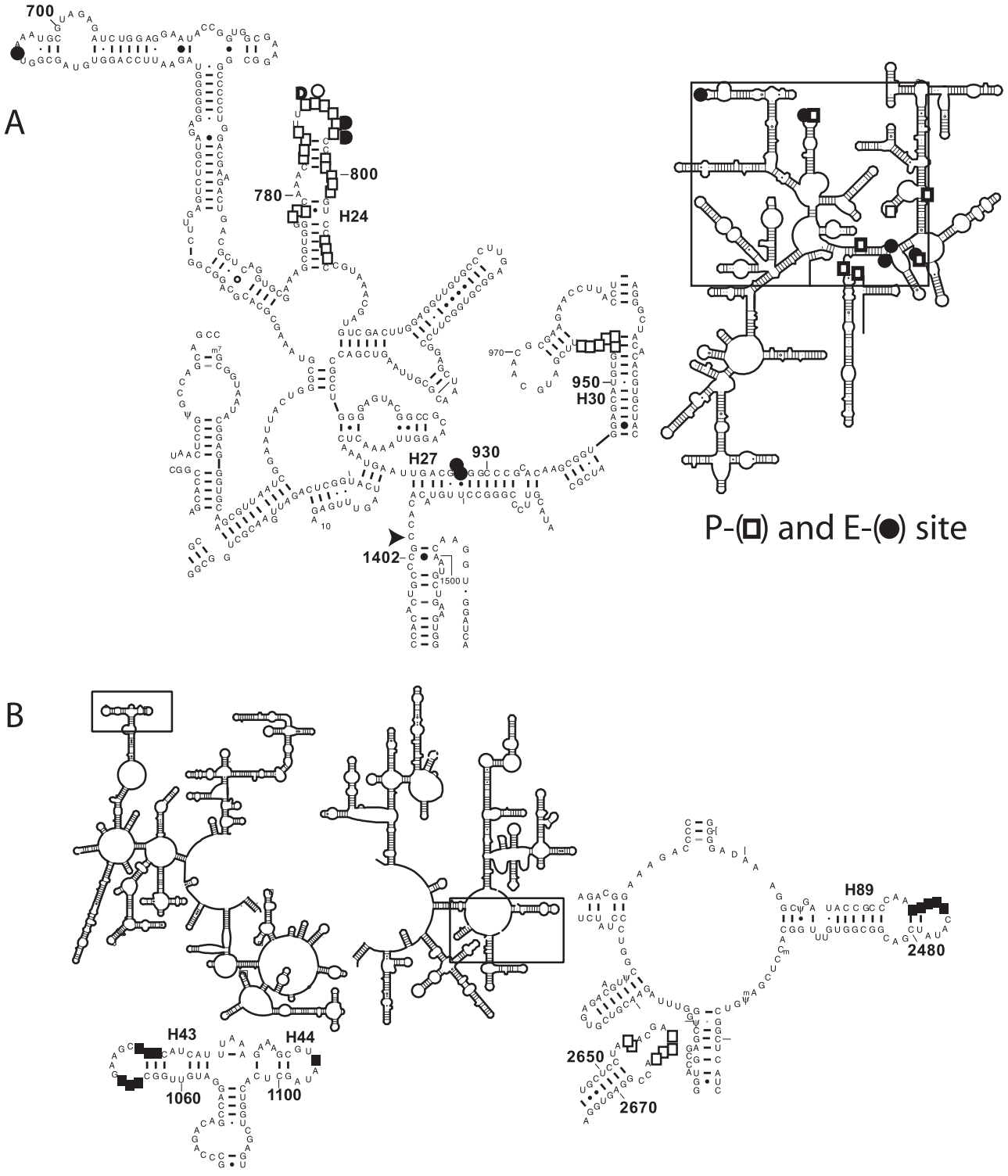

Figure 2. A summary of SmpB-footprints in 16S (**A**) and 23S rRNA (**B**). Positions are shown that are protected from kethoxal (circle) or DMS (half moon) modification or hydroxyl radical cleavage (square) in 30S or 50S subunits (open symbols) or in both subunits and ribosomes (filled symbols). The exposed base C1400 in 16S rRNA is indicated by an arrow. Secondary structure models are from (49). The inset in (A) shows interaction sites of P- (open squares) and E- (black circles) site tRNAs in 16S rRNA (1).

SmpB-footprints on helix H24 form a continuous surface on its solvent-exposed side, indicating a strong binding site of SmpB on the free 30S subunit in this region of 16S rRNA. The SmpB protection of nt 954–959, linking helices H30–H31, is too far away from the footprint on helix H24, to be explained by a direct contact with the same molecule of SmpB. Instead, SmpB binding may induce conformational changes in the 30S subunit that lead to the protection of the

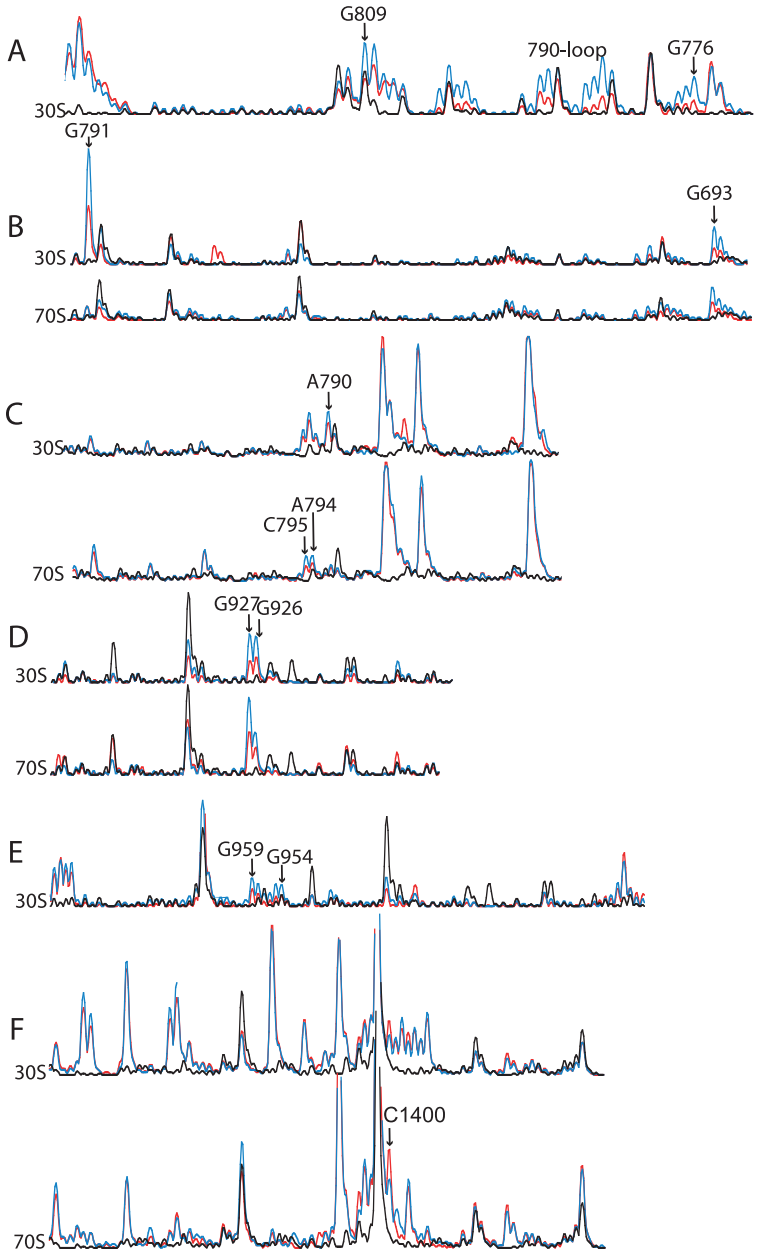

Figure 3. SmpB protects nucleotides in 16S rRNA from chemical modification and hydroxyl radical cleavage. The fluorograms show the reactive nucleotides in SmpB•30S or SmpB•70S complexes (red lines) and empty 30S subunits and 70S ribosomes (blue lines). Complexes were formed as described in Materials and Methods and cleaved with hydroxyl radicals (**A** and **E**) or modified with kethoxal (**B** and **D**) or DMS (**C** and **F**). Control samples (black lines) without added modifying reagent were run in parallel.

phosphate-backbone in the 954–959 region of 16S rRNA. Alternatively a second, partially filled SmpB-binding site is lost upon the formation of 70S ribosomes.

When the SmpB-footprints are compared with tRNA interaction sites in the 70S ribosome (1,3) almost all footprints on the 30S subunit are in the vicinity of the P-site facing the E-site (Figure 5A). The only exception is the exposed nt C1400 that is in the middle of the P-site. This is clearly shown in Figure 5A, where the A-site tRNA is yellow and the view is along the AC stem into the decoding cleft. The data thus suggest that SmpB binds in the vicinity of the P-site of the empty 30S subunit.

In 23S rRNA, the SmpB-footprinted nucleotides in the 1070-, 1095-, 2470- and 2660-regions (Figure 5B) are located below the L7/L12-stalk of the 50S subunit (3). It is evident that the protected nucleotides in the 1070- and 1095-regions are situated very close to the protected nucleotides in the apical loop of helix H89. Moreover, the sugar–phosphate backbone of the footprinted nucleotides forms a continuous patch on the solvent-accessible surface of 23S rRNA. It remains protected by SmpB not only in the free 50S subunit but also in the 70S ribosome, suggesting that there is a binding site of SmpB in this area of the 50S subunit. The footprint on the α-sarcin/ricin-loop is clearly separated from the other footprints in the

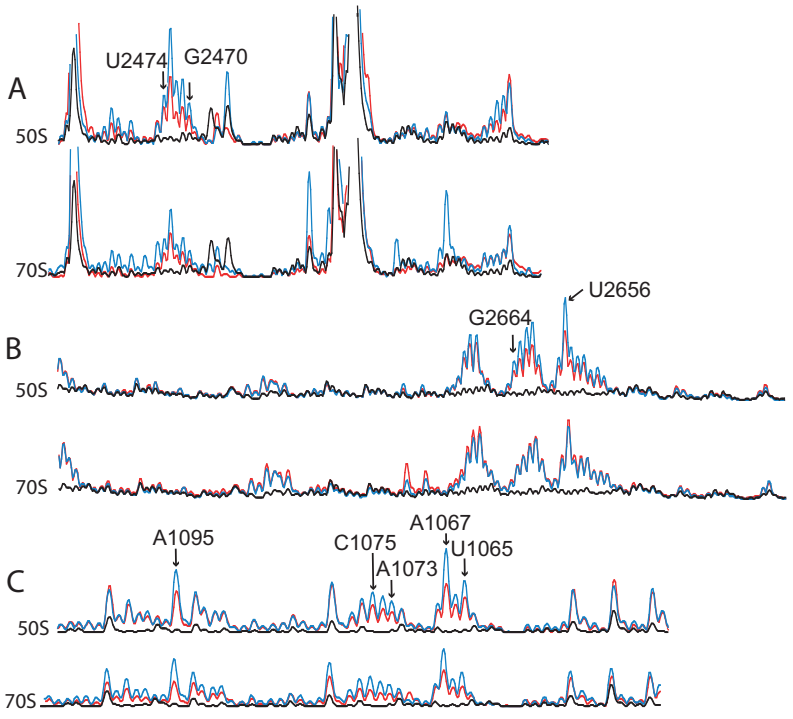

Figure 4. SmpB protects nucleotides from hydroxyl radical cleavage in 23S rRNA. The fluorograms show the reactive nucleotides in SmpB•50S or SmpB•70S complexes (red lines) and empty 50S subunits and 70S ribosomes (blue lines) in the (**A**) 2470-region (**B**) α-sarcin/ricin-loop and (**C**) 1070-region. Refer to the legend of Figure 3 for more details.

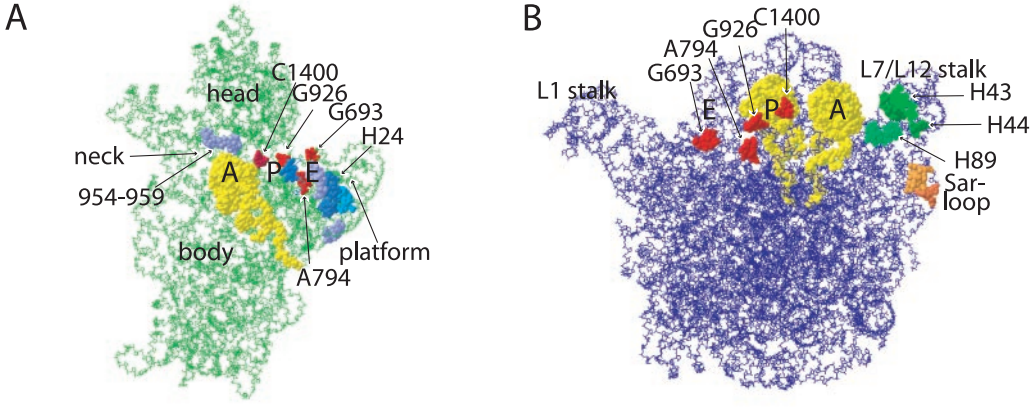

Figure 5. Mapping of SmpB-footprinted nucleotides on the 3D structure of the ribosome. (**A**) Nucleotides in 16S rRNA protected by SmpB bound to the free 30S subunit (painted blue, purple and red) and to the 70S ribosome (red). (**B**) Nucleotides in 23S rRNA protected by SmpB in the free 50S subunit (green and orange) and in the 70S ribosome (green) shown together with the positions of 16S rRNA protected in the 70S ribosome (red). The A-site (A and B) and P-site (B) tRNAs are painted in yellow and the A-, P- and E-sites are indicated. Both subunits are shown from the interface side. The location of the head, body, neck and platform are indicated on the 30S subunit (A) and the location of the L1 and L7/L12 stalks are indicated on the 50S subunit (B). The 3D structures of the *E.coli* 16S rRNA and 23S rRNA are from the 1PNS and 1PNU PDB files. Nucleotide positions are given in *E.coli* sequence numbering, which differs from that used in the 1PNS and 1PNU PDB files.

3D structure (Figure 5B), but may all the same come from a direct interaction of SmpB, since the distance between the two regions is <20 Å (3).

To find out whether the footprints in the 70S ribosome were the result of the interaction of one or more molecules of SmpB with the ribosome, the distances between footprinted nucleotides in the two subunits were measured. The two closest regions, footprinted in the 70S ribosome, are the 790-loop in 16S rRNA and helix H89 in 23S rRNA, and these are >70 Å apart in the crystal structure of the 70S ribosome (3). Therefore, the footprinting results suggest two different binding sites for SmpB on the 70S ribosome that may be occupied by two molecules of SmpB during *trans*-translation.

Effect of SmpB on translational accuracy

Finally, we tested whether the presence of SmpB on a 70S ribosome affects the accuracy of codon reading. For this, the effective association rate constants (k_{cat}/K_m) for the formation of fMet-Leu dipeptides by binding of Leu-tRNA$^{Leu}_{GAG}$ in ternary

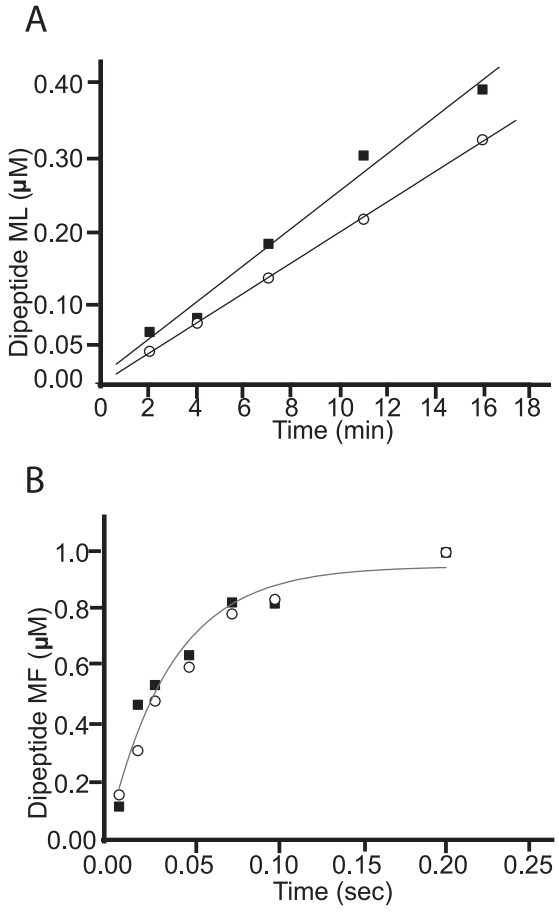

Figure 6. The figure represents the concentration of dipeptide (μM) formed on near-cognate (**A**) and on cognate (**B**) codon in the reaction mixture as a function of time. Circles, ribosomes with SmpB; squares, ribosomes without SmpB. Refer to Materials and Methods for more details.

complex with EF-Tu and GTP to initiated ribosomes programmed with the UUU codon in the A-site were determined. The ribosome activity was in each case checked by quantification of the amount of fMet-Phe dipeptide formed per ribosome when Leu-tRNA$^{Leu}_{GAG}$ in the reaction mixture was substituted for the cognate Phe-tRNA^{Phe}. The measured ribosome activity was typically 80–90%. We also determined k_{cat}/K_m for the cognate reaction of fMet-Phe dipeptide formation. All experiments were carried out with an *in vitro* system with components of high purity (41). The results reveal a small but significant increase in the accuracy of codon reading by the presence of SmpB (Figure 6). The k_{cat}/K_m value for the near-cognate codon reading was 98 M^{-1} s^{-1} in the presence and 142 M^{-1} s^{-1} in the absence of SmpB, while the cognate k_{cat}/K_m value was unaffected by the presence or absence of SmpB.

DISCUSSION

Here, we show that the 70S ribosome binds two molecules of SmpB in agreement with earlier data (24). The footprinting data suggest that one binding site is in the neck region of the 30S subunit close to the 30S P-site. The other binding site, on the 50S subunit, is close to the factor-binding site and to the so-called GAC, composed of helices H43 and H44 and r-protein L11. The data also show that several SmpB protected sites that are present on either one of the isolated subunits disappear in the 70S ribosome.

In 16S rRNA, these sites are often involved in inter-subunit contacts. Thus, the DMS reactivity of A790, the kethoxal reactivity of G791 as well as the hydroxyl radical footprints in helix H24 and the connecting 790-loop disappear upon subunit–subunit association (40). This makes it more difficult to evaluate the SmpB binding to the 790-region in 16S rRNA in the 70S ribosome. However, base-specific SmpB-footprints are still seen at positions 794 and 795, suggesting that SmpB interacts with this region of 16S rRNA in the 70S ribosome. Moreover, SmpB still footprints the 690-loop and nucleotides G926 and G927 in the 70S ribosome with no additional footprints detected elsewhere in 16S rRNA, indicating that the binding of SmpB is not shifted on the 70S ribosome compared with the 30S subunit. Altogether, this suggests that SmpB interacts with similar regions in the 70S ribosome and the 30S subunit, although the interaction with the former must be perturbed by the subunit–subunit bridge B2b formed by the 790-loop and helices 69 and 71 in 23S rRNA (1).

In contrast, in 23S rRNA, SmpB-footprints disappear in the α-sarcin/ricin-loop even though this loop is not involved in 70S formation (Figure 4B) (40). In the apical loop of helix H44, which is part of the GAC, the SmpB-footprints are stronger in the 70S ribosome than in the 50S subunit. This suggests a small shift of the SmpB-binding site on the 50S subunit towards the GAC, when the 70S ribosome is formed.

There is a small but significant increase in the accuracy of codon reading by the presence of SmpB on the ribosome (Figure 6). This effect is much smaller than the large accuracy changes induced by the presence of antibiotics or restrictive mutations in r-protein S12 (42–44). This shows that SmpB affects A-site-related processes even though our footprinting results do not suggest that SmpB binds to the 30S A-site of the ribosome. However, it is possible that it is the 50S-bound SmpB that affects translation accuracy by subtly changing the interaction of ternary complexes with the GAC on the 50S subunit of the ribosome.

A comparison of the SmpB-footprints in 16S rRNA with the interaction sites of P- and E-site bound tRNAs (Figure 2A) show that SmpB footprints nucleotides that are normally interacting with the ASLs of P- and E-site bound tRNAs (positions 34–39, where 35–37 is the anticodon). These sites overlap on the 30S subunit (1,45). The data presented here support a model where SmpB could functionally substitute an absent ASL of tmRNA when peptidyl-tmRNA subsequently moves into the P- and E-site of the 30S subunit. Interestingly, the N-3 position of C1400 that is situated in the P-site of the 30S subunit is more susceptible to methylation by DMS when SmpB is bound to the ribosome. At the same time, SmpB footprints G926, i.e. ∼10 Å, from C1400 in the 3D model of 16S rRNA (3). This suggests that SmpB binds in close proximity to the ribosomal P-site and affects its conformation. This notion is supported by the observation that SmpB footprints nt A790 and G791 (in the 790-loop) in the 30S subunit. Formation of bridge B2b in the 70S ribosome or interaction of the ASL of P-site bound tRNA with the backbone in the

790-loop stabilize the interaction between bases A790 and G791 and the backbone at positions 1497–1498 in 16S rRNA (1,46).

We suggest that SmpB may favour similar interactions in the empty 30S subunit. Furthermore, SmpB may stabilize the post-translocation peptidyl-tmRNA•SmpB•ribosome complex, thereby ensuring an accurate shift in codon reading from the mRNA to the tmRNA mode. In addition, SmpB may be important for rapid translocation of tmRNA from the A- to the P-site and then from the P- to the E-site by making up for missing interactions, between tmRNA and the ribosomal P-site that are important for translocation of tRNAs (47,48).

The footprints in the apical loop of H89 and in helices H43 and H44 in the 50S subunit are consistent with the SmpB-positioning in the cryo-EM structure of the complex between Ala-tmRNA and 70S ribosomes in the presence of EF-Tu•GDP•Kirromycin (15). In this complex, SmpB is modelled in the electron density map so that it simultaneously contacts the TLD and the apical loop of helix H89 and is in close proximity to helices H69 and H71 in domain IV of 23S rRNA (15). Our footprints in the H89 helix are in general agreement with the proposed placement of SmpB in the cryo-EM structure. However, the absence of SmpB-footprints on helices 69 and 71, both in the free 50S subunit and in the 70S ribosome, indicates that the actual SmpB-binding site on the 50S subunit should be located closer to the 1070- and 1095-loops than in the cryo-EM reconstruction (19).

The probable binding site of SmpB on the 30S subunit, presented here, can be compared with the proposal by Gutmann *et al*. (22). In their model, based on docking of the crystal structure of the SmpB•TLD complex into the structure of the 70S ribosome in complex with the A-site tRNA (1), SmpB is oriented towards the A-site of the small subunit. In contrast, our data suggest that SmpB binds close to the P-site, rather than to the A-site of the 30S subunit. One reason for this discrepancy could be that the A-site positioning of SmpB requires the presence of tmRNA on the ribosome and that it occurs only after Ala-tmRNA accommodation in the A-site of the 50S subunit.

Our results show that purified SmpB binds to both 30S and 50S particles in 1:1 molar ratios and to 70S ribosomes in a 2:1 molar ratio. The mapping of the SmpB-footprinted nucleotides on the crystal structure of the 70S ribosome shown in Figure 5 indicates that it is highly unlikely that one SmpB molecule could account for footprints both in the platform region of the 30S subunit and for the footprints below the L7/L12-stalk of the 50S subunit, since these two regions are more than 70 Å apart in the 70S crystal structure (1,3). Therefore, the footprinting data support the notion that two molecules of SmpB bind to the empty 70S ribosome. SmpB bound to the 30S subunit was not observed by cryo-EM (15). One explanation similar to that of Gutman *et al*. (22) could be that SmpB moves from its 50S location (15) to the 30S location concomitantly with the accommodation of Ala-tmRNA in the A-site of the 50S subunit or, more probably, at a later stage in *trans*-translation after translocation of the peptidyl-tmRNA into the P-site as discussed above. For example, it could be that the 50S footprint corresponds to the entry to and the 30S footprint to the exit from the ribosome of the TLD domain of tmRNA in complex with SmpB. However, in order for the 50S-oriented SmpB in the pre-accommodation cryo-EM-structure of the SmpB•Tu•GDP•Ala-tmRNA complex to become oriented towards the A-site in the post-accommodation state as in the model by Gutman *et al*. (22), the D-loop of tmRNA through which SmpB binds to tmRNA must rotate by more than 100° with respect to the orientation of the acceptor stem of tmRNA. This huge conformational change in tmRNA upon its A-site accommodation is hardly feasible. Therefore, we suggest an alternative that involves two molecules of SmpB. One remains bound to the 50S subunit as in the cryo-EM reconstruction (15), while the other SmpB molecule is bound to tmRNA, as in the docking model by Gutmann *et al*. (22). The latter SmpB molecule subsequently follows tmRNA as it moves from site to site on the ribosome during *trans*-translation. It could functionally substitute for the missing ASL of tmRNA, as it moves from A- to P- to E-site and thus be responsible for the observed footprints on the 30S subunit. The strong footprints we observe in the P-site of the 30S subunit may reflect the relatively strong affinity of SmpB for the small ribosomal subunit (Figure 1). This binding energy could be the key to how SmpB facilitates translocation of tmRNA from the A- to the P-site. In summary, we suggest that two SmpB molecules participate in *trans*-translation, one facilitating the interaction of tmRNA with the 50S subunit and the other facilitating the tmRNA interaction with the 30S subunit. The 30S-oriented SmpB molecule could simply have been missed in the cryo-EM reconstruction, due to the relatively low resolution (13–15 Å) of the electron density map in this study (15). Future experiments will be required to discriminate between the one- and the two-SmpB scenarios in *trans*-translation.

ACKNOWLEDGEMENTS

L.H.S. thanks Odd Nygård for general support. This work was supported by grants from the Swedish Research Council to L.H.S. and M.E. Funding to pay the Open Access publication charges for this article was provided by Södertörns Högskola.

Conflict of interest statement. None declared.

REFERENCES

1. Yusupov,M.M., Yusupova,G.Z., Baucom,A., Lieberman,K., Earnest,T.N., Cate,J.H. and Noller,H.F. (2001) Crystal structure of the ribosome at 5.5 A resolution. *Science*, **292**, 883–896.
2. Rheinberger,H.J., Sternbach,H. and Nierhaus,K.H. (1981) Three tRNA binding sites on *Escherichia coli* ribosomes. *Proc. Natl Acad. Sci. USA*, **78**, 5310–5314.
3. Vila-Sanjurjo,A., Ridgeway,W.K., Seymaner,V., Zhang,W., Santoso,S., Yu,K and Cate,J.H. (2003) X-ray crystal structures of the WT and a hyper-accurate ribosome from *Escherichia coli*. *Proc. Natl Acad. Sci. USA*, **100**, 8682–8687.
4. Ramakrishnan,V. (2002) Ribosome structure and the mechanism of translation. *Cell*, **108**, 557–572.
5. Keiler,K.C., Waller,P.R. and Sauer,R.T. (1996) Role of a peptide tagging system in degradation of proteins synthesized from damaged messenger RNA. *Science*, **271**, 990–993.
6. Atkins,J.F. and Gesteland,R.F. (1996) A case for trans translation. *Nature*, **379**, 769–771.
7. Komine,Y., Kitabatake,M., Yokogawa,T., Nishikawa,K. and Inokuchi,H. (1994) A tRNA-like structure is present in 10Sa RNA, a small stable RNA from *Escherichia coli*. *Proc. Natl Acad. Sci. USA*, **91**, 9223–9227.

8. Ushida,C., Himeno,H., Watanabe,T. and Muto,A. (1994) tRNA-like structures in 10Sa RNAs of Mycoplasma capricolum and *Bacillus subtilis*. *Nucleic Acids Res*., **22**, 3392–3396.
9. Tu,G.F., Reid,G.E., Zhang,J.G., Moritz,R.L. and Simpson,R.J. (1995) C-terminal extension of truncated recombinant proteins in *Escherichia coli* with a 10Sa RNA decapeptide. *J. Biol. Chem*., **270**, 9322–9326.
10. Keiler,K.C. and Sauer,R.T. (1996) Sequence determinants of C-terminal substrate recognition by the Tsp protease. *J. Biol. Chem*., **271**, 2589–2593.
11. Rudinger-Thirion,J., Giege,R. and Felden,B. (1999) Aminoacylated tmRNA from *Escherichia coli* interacts with prokaryotic elongation factor Tu. *RNA*, **5**, 989–992.
12. Barends,S., Karzai,A.W., Sauer,R.T., Wower,J. and Kraal,B. (2001) Simultaneous and functional binding of SmpB and EF-Tu-TP to the alanyl acceptor arm of tmRNA. *J. Mol. Biol*., **314**, 9–21.
13. Barends,S., Wower,J. and Kraal,B. (2000) Kinetic parameters for tmRNA binding to alanyl-tRNA synthetase and elongation factor Tu from *Escherichia coli*. *Biochemistry*, **39**, 2652–2658.
14. Hanawa-Suetsugu,K., Takagi,M., Inokuchi,H., Himeno,H. and Muto,A. (2002) SmpB functions in various steps of trans-translation. *Nucleic Acids Res*., **30**, 1620–1629.
15. Valle,M., Gillet,R., Kaur,S., Henne,A., Ramakrishnan,V. and Frank,J. (2003) Visualizing tmRNA entry into a stalled ribosome. *Science*, **300**, 127–130.
16. Karzai,A.W., Roche,E.D. and Sauer,R.T. (2000) the SsrA-SmpB system for protein tagging, directed degradation and ribosome rescue. *Nature Struct. Biol*., **7**, 449–455.
17. Karimi,R., Pavlov,M.Y., Buckingham,R.H. and Ehrenberg,M. (1999) Novel roles for classical factors at the interface between translation termination and initiation. *Mol. Cell*, **3**, 601–609.
18. Shimizu,Y. and Ueda,T. (2002) The role of SmpB protein in trans-translation. *FEBS Lett*., **514**, 74–77.
19. Dong,G., Nowakowski,J. and Hoffman,D.W. (2002) Structure of small protein B: the protein component of the tmRNA-SmpB system for ribosome rescue. *EMBO J*., **21**, 1845–1854.
20. Someya,T., Nameki,N., Hosoi,H., Suzuki,S., Hatanaka,H., Fujii,M., Terada,T., Shirouzu,M., Inoue,Y., Shibata,T. *et al*. (2003) Solution structure of a tmRNA-binding protein, SmpB, from *Thermus thermophilus*. *FEBS Lett*., **535**, 94–100.
21. Jacob,Y., Sharkady,S.M., Bhardwaj,K., Sanda,A.A. and Williams,K.P. (2005) Function of the SmpB tail in tmRNA translation revealed by a nucleus-encoded form. *J. Biol. Chem*., **280**, 5503–5509.
22. Gutmann,S., Haebel,P.W., Metzinger,L., Sutter,M., Felden,B. and Ban,N. (2003) Crystal structure of the transfer-RNA domain of transfer-messenger RNA in complex with SmpB. *Nature*, **424**, 699–703.
23. Wower,J., Zwieb,C.W., Hoffman,D.W. and Wower,I.K. (2002) SmpB: a protein that binds to double-stranded segments in tmRNA and tRNA. *Biochemistry*, **41**, 8826–8836.
24. Hallier,M., Ivanova,N., Rametti,A., Pavlov,M., Ehrenberg,M. and Felden,B. (2004) Pre-binding of small protein B to a stalled ribosome triggers trans-translation. *J. Biol. Chem*., **279**, 25978–25985.
25. Shpanchenko,O.V., Zvereva,M.I., Ivanov,P.V., Bugaeva,E.Y., Rozov,A.S., Bogdanov,A.A., Kalkum,M., Isaksson,L.A., Nierhaus,K.H. and Dontsova,O.A. (2005) Stepping tmRNA through the ribosome. *J. Biol. Chem*., **280**, 18368–18374.
26. Metzinger,L., Hallier,M. and Felden,B. (2005) Independent binding sites of small protein B onto transfer-messenger RNA during *trans*-translation. *Nucleic Acids Res*., **33**, 2384–2394.
27. Ivanova,N., Pavlov,M.Y., Felden,B. and Ehrenberg,M. (2004) Ribosome rescue by tmRNA requires truncated mRNAs. *J. Mol. Biol*., **338**, 33–41.
28. Pavlov,M.Y., Freistroffer,D.V., MacDougall,J., Buckingham,R.H. and Ehrenberg,M. (1997) Fast recycling of *Escherichia coli* ribosomes requires both ribosome recycling factor (RRF) and release factor RF3. *EMBO J*., **16**, 4134–4141.
29. Antoun,A., Pavlov,M., Tenson,T. and Ehrenberg,M. (2004) Ribosome formation from subunits studied by stopped-flow and Rayleigh light scattering. *Biol. Proced. Online*, **6**, 35–54.
30. Gillam,I., Millward,S., Blew,D., von Tigerstrom,M., Wimmer,E. and Tener,G.M. (1967) The separation of soluble ribonucleic acids on benzoylated diethylaminoethylcellulose. *Biochemistry*, **6**, 3043–3056.
31. Ehrenberg,M., Bilgin,N. and Kurland,C. (1990) Design and use of a fast and accurate in vitro translation system.. In Spedding,G. (ed.), *Ribosomes and Protein Synthesis. A Practical Approach*. IRL Press at Oxford University Press, Oxford, UK, pp. 101–129.
32. Holmberg,L. and Noller,H.F. (1999) Mapping the ribosomal RNA neighborhood of protein L11 by directed hydroxyl radical probing. *J. Mol. Biol*., **289**, 223–233.
33. Moazed,D. and Noller,H.F. (1989) Intermediate states in the movement of transfer RNA in the ribosome. *Nature*, **342**, 142–148.
34. Rodnina,M.V. and Wintermeyer,W. (1995) GTP consumption of elongation factor Tu during translation of heteropolymeric mRNAs. *Proc. Natl Acad. Sci. USA*, **92**, 945–949.
35. Jelenc,P.C. and Kurland,C.G. (1979) Nucleoside triphosphate regeneration decreases the frequency of translation errors. *Proc. Natl Acad. Sci. USA*, **76**, 3174–3178.
36. Merryman,C. and Noller,H.F. (1998) *Footprinting and Modification-Interference Analysis of Binding Sites on RNA*. Oxford University Press, Oxford.
37. Larsson,S.L. and Nygård,O. (2001) Proposed secondary structure of eukaryote specific expansion segment 15 in 28S rRNA from mice, rats, and rabbits. *Biochemistry*, **40**, 3222–3231.
38. Knutsson Jenvert,R.-M. and Holmberg Shiavone,L. (2005) Characterization of the tRNA and ribosome-dependent pppGpp-synthesis by recombinant stringent factor from *Escherichia coli*. *FEBS J*., **272**, 685–695.
39. Pavlov,M.Y., Freistroffer,D.V., Heurgue-Hamard,V., Buckingham,R.H. and Ehrenberg,M. (1997) Release factor RF3 abolishes competition between release factor RF1 and ribosome recycling factor (RRF) for a ribosome binding site. *J. Mol. Biol*., **273**, 389–401.
40. Merryman,C., Moazed,D., McWhirter,J. and Noller,H.F. (1999) Nucleotides in 16S rRNA protected by the association of 30S and 50S ribosomal subunits. *J. Mol. Biol*., **205**, 97–105.
41. Pavlov,M.Y. and Ehrenberg,M. (1996) Rate of translation of natural mRNAs in an optimized *in vitro* system. *Arch. Biochem. Biophys*., **328**, 9–16.
42. Bilgin,N., Claesens,F., Pahverk,H. and Ehrenberg,M. (1992) Kinetic properties of *Escherichia coli* ribosomes with altered forms of S12. *J. Mol. Biol*., **224**, 1011–1027.
43. Weiser,J., Ehrenberg,M. and Naprstek,J. (1994) *In vitro* measurement of translation accuracy of ribosomes isolated from streptomycin-resistant mutant of *Streptomyces granaticolor*. *Folia Microbiol. (Praha)*, **39**, 129–132.
44. Björkman,J., Samuelsson,P., Andersson,D.I. and Hughes,D. (1999) Novel ribosomal mutations affecting translational accuracy, antibiotic resistance and virulence of *Salmonella typhimurium*. *Mol. Microbiol*., **31**, 53–58.
45. Moazed,D. and Noller,H.F. (1989) Interaction of tRNA with 23S rRNA in the ribosomal A, P, and E sites. *Cell*, **57**, 585–597.
46. Moazed,D. and Noller,H.F. (1986) Transfer RNA shields specific nucleotides in 16S rRNA from attack by chemical probes. *Cell*, **47**, 985–994.
47. Joseph,S. and Noller,H.F. (1998) EF-G-catalyzed translocation of anticodon stem-loop analogs of transfer RNA in the ribosome. *EMBO J*., **17**, 3478–3483.
48. Phelps,S.S., Jerinic,O. and Joseph,S. (2002) Universally conserved interactions between the ribosome and the anticodon stem-loop of A site tRNA important for translocation. *Mol. Cell*., **10**, 799–807.
49. Cannone,J.J., Subramanian,S., Schnare,M.N., Collett,J.R., D'Souza,L.M., Du,Y., Feng,B., Lin,N., Madabusi,L.V., Muller,K.M. *et al*. (2002) The comparative RNA web (CRW) site: an online database of comparative sequence and structure information for ribosomal, intron, and other RNAs. *BioMed. Central Bioinformatics*, **3**, 2.